PHYSICS OF FLUIDS **25**, 091701 (2013)

Experimental evidence of the modulation of a plane wave to oblique perturbations and generation of rogue waves in finite water depth

A. Toffoli,[1,2] L. Fernandez,[3] J. Monbaliu,[3] M. Benoit,[4] E. Gagnaire-Renou,[4] J. M. Lefèvre,[5] L. Cavaleri,[6] D. Proment,[7] C. Pakozdi,[8] C. T. Stansberg,[8] T. Waseda,[9] and M. Onorato[10,11]
[1]*School of Marine Science and Engineering, Plymouth University, Plymouth PL4 8AA, United Kingdom*
[2]*Centre for Ocean Engineering Science and Technology, Swinburne University of Technology, P.O. Box 218, Hawthorn, Victoria 3122, Australia*
[3]*Department of Civil Engineering, KU Leuven, Kasteelpark Arenberg 40, Box 2448, 3001 Heverlee, Belgium*
[4]*Saint-Venant Laboratory for Hydraulics, Université Paris-Est (Joint Research Unit EDF R&D, CETMEF, Ecole des Ponts ParisTech), 6 quai Watier, BP 49, 78401 Chatou, France*
[5]*Division Marine et Oceanographie, Meteo-France, 42 av G. Coriolis, 31057 Toulouse, France*
[6]*Institute of Marine Sciences, Castello 2737/F, 30122 Venice, Italy*
[7]*School of Mathematics, University of East Anglia, Norwich NR4 7TJ, United Kingdom*
[8]*Marintek, P.O. Box 4125, Valentinlyst, N-7450 Trondheim, Norway*
[9]*Graduate School of Frontier Sciences, University of Tokyo, Kashiwa, Chiba 277-8563, Japan*
[10]*Dipartimento di Fisica, Universita di Torino, Via P. Giuria, Torino 10125, Italy*
[11]*INFN, Sezione di Torino, Via Pietro Giuria 1, 10125 Torino, Italy*

(Received 19 June 2013; accepted 3 September 2013; published online 20 September 2013)

We present a laboratory experiment in a large directional wave basin to discuss the instability of a plane wave to oblique side band perturbations in finite water depth. Experimental observations, with the support of numerical simulations, confirm that a carrier wave becomes modulationally unstable even for relative water depths $k_0h < 1.36$ (with k the wavenumber of the plane wave and h the water depth), when it is perturbed by appropriate oblique disturbances. Results corroborate that the underlying mechanism is still a plausible explanation for the generation of rogue waves in finite water depth. © *2013 AIP Publishing LLC*. [http://dx.doi.org/10.1063/1.4821810]

The generation of very large amplitude waves (also known as freak or rogue waves) has received much attention during the past decades in many different fields of physics, including hydrodynamics,[1–4] nonlinear optics,[5,6] and plasma physics[7] (see a general overview in Onorato *et al.*[8]). One of the most accredited mechanisms responsible for the generation of deep water rogue waves is the modulation of wave packets due to unstable perturbations.[9–11] This is a generalisation of the Benjamin–Feir or modulational instability,[12] which leads to strong focussing of wave energy through a quasi-resonant four-wave interaction process. At cubic order, the instability of deep water waves is described by the nonlinear Schrödinger equation[13] (NLS), which is derived from the Euler equations by assuming that waves are weakly nonlinear (i.e., steepness $\varepsilon = k_0a_0 \ll 1$, where k_0 is the wavenumber of the carrier wave and a_0 is its amplitude) and have narrow bandwidth ($\Delta k/k_0 \ll 1$, where Δk is the modulation wavenumber). For collinear propagation (i.e., carrier wave and disturbances have the same direction), a linear stability analysis of NLS indicates that unstable disturbances can lead to an exponential growth of a small-amplitude modulation.[14,15] Interestingly enough, laboratory experiments[16,17] and numerical simulations[14,18–20] suggest that a plane wave is also unstable to oblique side bands (i.e., disturbances propagating at an angle with respect to the carrier) if propagation in two horizontal dimensions is allowed. This is ensured by the fact that the region of instability (as derived from a 2+1 NLS) is stretched over a narrow domain forming an angle

1070-6631/2013/25(9)/091701/7/$30.00

of about 35.5° with the mean wave direction. In wavenumber space, this corresponds to $\Delta k_y/\Delta k_x \approx 0.7$, where Δk_x and Δk_y are the components of the oblique modulation wavenumber in the (k_x, k_y) plane[21] (see the nonlinear instability diagram in Fig. 16 of Kharif and Pelinovsky,[10] for example). Although the modulation is primarily dominated by collinear perturbations in infinite water depth ($k_0 h \to \infty$, where h is the water depth),[22] the most unstable modes are normally oblique with respect to the carrier wave in arbitrary water depths ($k_0 h \le \varepsilon^{-1}$).[18,22] Direct numerical simulations of a 2+1 NLS equation,[14,20] in this regard, confirm that oblique disturbances are also capable of triggering an exponential growth of a small-amplitude modulation and hence rogue waves.

It is worth noting that many observations of extreme waves in the ocean have been reported in conditions of finite water depths (normally $k_0 h < 2$),[23–26] including the famous Draupner wave.[23,24] For $k_0 h \approx O(1)$, the interaction with the sea floor generates a wave-induced current that subtracts energy from nonlinear focussing and, as a consequence, attenuates the modulation of wave trains to side band perturbations. It follows that the instability diagram shrinks with decreasing depth, concentrating gradually over a very narrow region of constant $\Delta k_y/\Delta k_x \approx 0.7$ for $k_0 h \ge 1.36$ and increasing to $\Delta k_y/\Delta k_x \approx 0.77$ as $k_0 h$ approaches the value of 1.[10,22] Under these circumstances, a plane wave remains stable under the influence of a collinear perturbations for $k_0 h \le 1.36$, while it can still destabilise under the effect of oblique unstable modes.[20,27–33] Apart from the generation of crescent waves,[31–33] numerical simulations based on the 2+1 NLS suggest that oblique side bands can still lead to the formation of rogue waves also for $k_0 h < 1.36$ (see Slunyaev *et al.*[20]). Despite its importance in many fields of physics and earth science, however, this result has not received a proper experimental confirmation yet.

In the present letter, we discuss a set of laboratory experiments that were carried out to investigate wave dynamics in finite water depth. The aim is to validate the conjecture that the modulation of plane wave by oblique perturbations can lead to rogue waves also when $k_0 h < 1.36$. Experiments were conducted in the directional ocean wave basin at MARINTEK (Norway), which is 70 m wide and 50 m long. The facility is equipped with 144 individually controlled flaps for the generation of directional wave components on the 70 m side and a unidirectional wavemaker on the 50 m one (only the former was used for the present study); absorbing beaches are mounted on the opposite side of each wavemaker. The water depth is uniform and controlled by a movable bottom, which was set to a depth $h = 0.78$ m for this specific experiment. The surface elevation was monitored by 25 capacitance gauges distributed along the basin at a sampling frequency of 200 Hz; three 3-probe arrays shaped as a triangle and one 6-probe array shaped as a pentagon with a probe in the middle were also deployed to monitor directional properties (a schematic diagram of the experiment is presented in Fig. 1). The instrumentation layout is similar to the one applied by Onorato *et al.*[34]

Initial conditions consisted in a sinusoidal (carrier) wave, which was seeded by 4 oblique side bands. Different configurations of the carrier wave were selected with period $T = 1$ s, 1.35 s, 1.68 s,

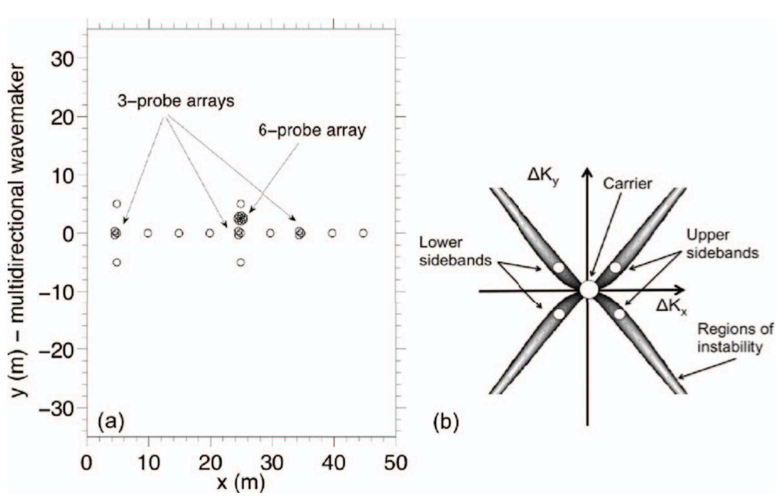

FIG. 1. Schematic representation of the experimental set up (a) and initial condition imposed at the wavemaker (b).

and 1.84 s, which defined relative water depths $k_0h = 3.15$, 1.78, 1.24, and 1.09, respectively. For brevity, here we will only present two cases: $k_0h = 1.78$ and 1.24. The related wave amplitudes were selected such that all tests ran with identical wave steepness $k_0a_0 = 0.14$. Perturbations were accurately chosen within the unstable region of the instability diagram. Specifically, two upper and two lower oblique disturbances with coordinates $[\Delta k_x, \Delta k_y]$, $[\Delta k_x, -\Delta k_y]$, $[-\Delta k_x, -\Delta k_y]$, and $[-\Delta k_x, \Delta k_y]$ were applied (see right panel in Fig. 1). The modulational wavenumber components along the mean wave direction (x) were selected by ensuring a number of 5 waves under the modulation in the physical space and thus about 10 waves in the time domain. Components in the transverse direction (y) were chosen such that $|\Delta k_y/\Delta k_x| = 0.6$ for $k_0h > 1.36$ and $|\Delta k_y/\Delta k_x| = 0.75$ for $k_0h < 1.36$. Tests were also repeated for collinear configurations (i.e., unidirectional propagation) by imposing $\Delta k_y = 0$. Each perturbation was then given a rather large amplitude (a_b) equivalent to 30% of the amplitude of the carrier wave. Note that this is related to the difficulties in replicating wave instability in finite water depth due to the large space scales that are required to fully develop the maximum wave amplification and the relatively short length of the facility. The selection of such large amplitudes coincides with an advanced stage of the modulation process, which is expected to have started under the effect of infinitesimal (small-amplitude) disturbances. The advantage of this configuration is the reduction of the space scale that is necessary for reaching the maximum amplification.

It is important to note that five-wave interaction (class II instability) may be triggered, owing to the high steepness of the carrier wave.[31–33] Nonetheless, here we focus on modulational-like instability as a result of four-wave interaction that is expected to play a major role in the generation of large waves. In order to provide a theoretical benchmark for the interpretation of the experimental results in this regard, we replicated laboratory observations with direct numerical simulations of the Euler equations, by applying the Higher Order Spectral Method (HOSM) proposed by West *et al*.[35] (details for the application of HOSM in finite water depth can be found, for example, in Toffoli *et al*.[36]). The method uses a series expansion in the wave slope of the vertical velocity to resolve the surface elevation and the velocity potential. Simulations have been performed with a third order expansion so that only four-wave interaction effects were enabled.[37] No dissipation term was applied.

One of the drawbacks of the numerical method is that it replicates the temporal evolution of an initial surface, while experiments describe the spacial evolution of an initial time series. To allow a comparison, we make the assumption that time can be translated into space by means of the group velocity. This approach has been successfully used to compare experimental data with HOSM simulations in Toffoli *et al*.[38] We stress, however, that the purpose of the numerical simulations is to support the interpretation of the experiments rather than provide a data set for a quantitative validation of the results.

The physical domain for the simulations was selected to cover a square footprint of 9 dominant waves along the mean direction of propagation. A grid of 256×256 points was used to ensure a fine computational mesh with 28 grid points per dominant wave. The time integration was performed with a time step $\Delta t = T/200$ s and covered a total time frame equivalent to 400 wave periods. The initial input surface was selected to resemble the input experimental conditions at the initial stage of the modulation process, i.e., a carrier wave perturbed by small-amplitude disturbances.

In spectral space, the four-wave interaction results in a nonlinear energy transfer from the carrier wave to the unstable side bands, with the lower ones growing faster than the upper disturbances.[39,40] Due to the closeness of wave modes, reconstruction of the two dimensional spectrum at the probe arrays did not provide a neat separation of the different directional components. A spectral analysis was therefore restricted to the frequency wave spectra as calculated from an individual wave gauge at different distances from the wavemaker (see Figs. 2 and 3 for $k_0h = 1.78$ and 1.24, respectively). Note, however, that this representation only shows a sum of the oblique disturbances at a given frequency. For $k_0h = 1.78$, as expected, we observed a rapid asymmetric growth of the side bands both in one and two dimensional propagation. There is, nonetheless, a energy loss for higher frequency components due to selective breaking towards the end of the basin, which is consistent with previous observations in, e.g., Tulin and Waseda.[40] For $k_0h < 1.36$, energy transfer ceases under the condition of unidirectional propagation, at least within the boundaries of the facility (see upper

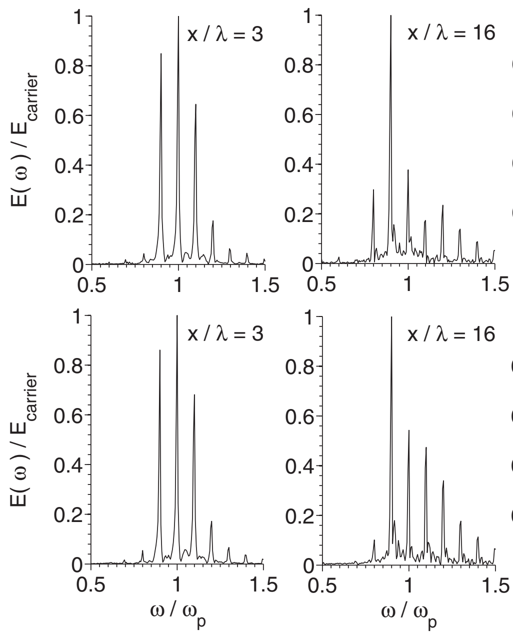

FIG. 2. Spectral evolution along the basin for relative water depth $k_0h = 1.78$: test with collinear perturbations (upper panels); test with oblique perturbations (lower panels).

panels in Fig. 3), in agreement with the suppression of modulational instability.[27] A certain degree of dissipation was, however, recorded along the basin as a result of bottom friction and depth-induced breaking. By allowing propagation in two horizontal dimensions, on the other hand, the imposed oblique perturbations trigger modulational instability and consequently a nonlinear energy transfer between the carrier and the perturbations. Under these circumstances, an asymmetric growth of the side bands was observed (see lower panel in Fig. 3). Although energy dissipation occurred due to

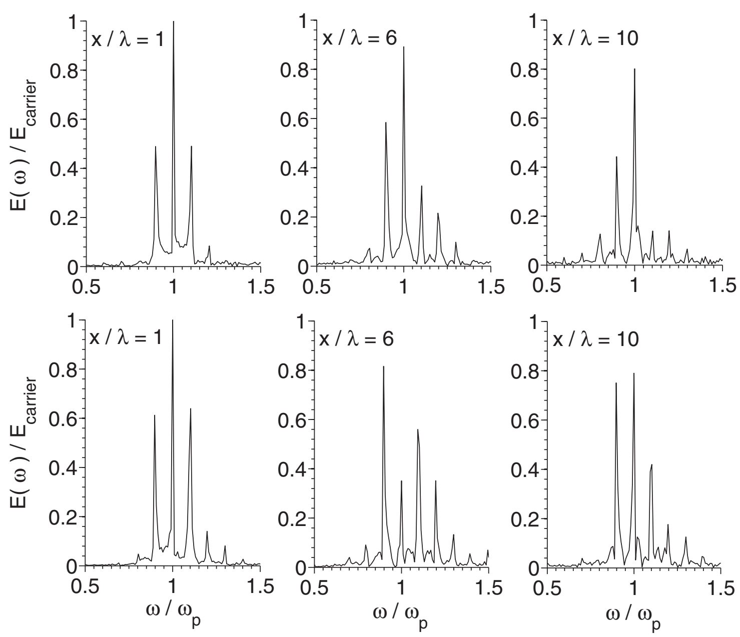

FIG. 3. Spectral evolution along the basin for relative water depth $k_0h = 1.24$: test with collinear perturbations (upper panels); test with oblique perturbations (lower panels).

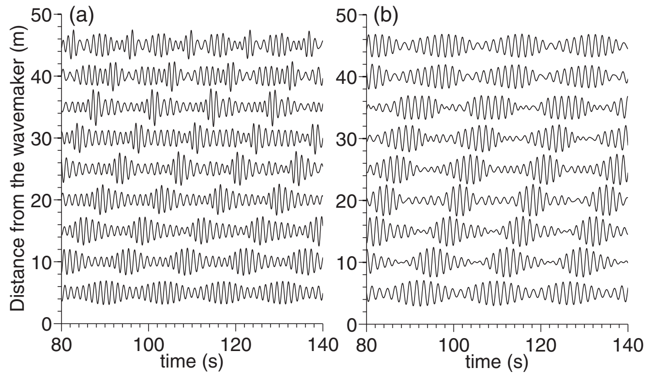

FIG. 4. Spatial evolution of a wave packed perturbed by an oblique modulation: (a) $kh = 1.78$; (b) $kh = 1.24$.

bottom friction and breaking, the initial spectral configuration tends to be restored towards the end of the basin. To some extent, the reported growth of oblique side bands is in agreement with previous laboratory experiments in a long flume,[16] where a uniform wave without seeding of unstable modes was observed to transferred energy towards a lower oblique sideband.

In the physical space, wave instability results in a nonlinear energy focussing, which makes the modulation more pronounced. This is highlighted in Fig. 4, where the evolution of a carrier wave perturbed by oblique side bands (for both $k_0h = 1.78$ and 1.24) is presented. As modulation instability only relates to free wave components, bound waves were filtered out by removing frequencies lower than 0.5 and larger than 1.5 times the peak frequency. The resulting time series indicate clearly the enhancement of wave modulation and the consequent amplitude growth. This is more pronounced for $k_0h = 1.78$, where waves become particularly steep and eventually start breaking towards the end of the basin.

In order to verify the conjecture that the observed wave amplification is the result of modulational instability, experimental observations were compared against numerical simulations. The normalised maximum wave amplitude at each probe is presented in Figs. 5 and 6 (for $k_0h = 1.78$ and 1.24, respectively) as a function of the normalised distance from the wavemaker. Bound waves were removed from both experimental and numerical records. The amplitude of the carrier wave is here used as normalising factor for the wave amplitude, while the wavelength λ is used for normalising the distance from the wavemaker. Note that the condition $x = 0$ corresponds to the stage of wave modulation that was imposed at the wavemaker. In this regard, it is important to remark that numerical simulations start from a condition of small-amplitude modulation, while experiments have been forced to begin at an advanced stage of instability to allow the underlying process to develop within the boundaries of the facility. Thus, the negative abscissa covers the initial part of the propagation, which is not accounted for in the experiments.

For $k_0h > 1.36$, numerical simulations show, as expected, that modulational instability induces a rapid and substantial growth of wave amplitude in both one and two dimensional propagation. It is

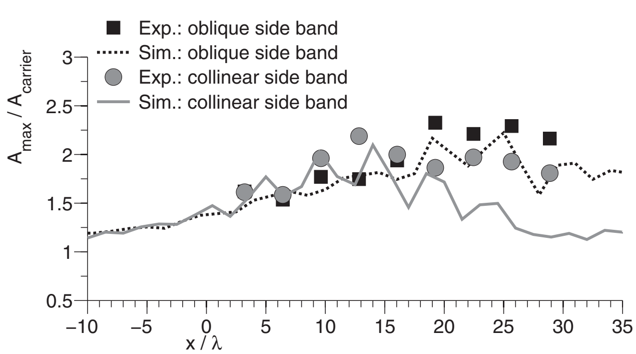

FIG. 5. Spacial evolution of the maximum wave amplitude for relative water depth $kh = 1.78$.

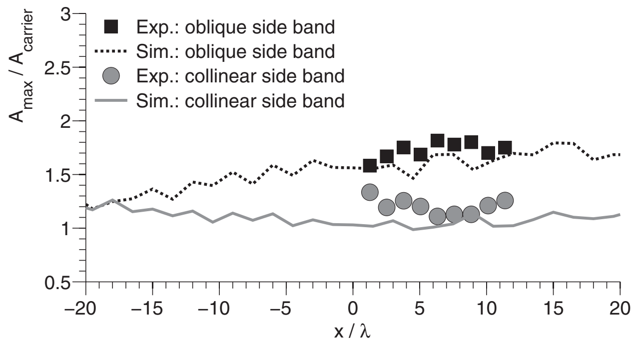

FIG. 6. Spacial evolution of the maximum wave amplitude for relative water depth $kh = 1.24$.

worth mentioning that wave growth is slightly quicker in the collinear (unidirectional) configuration, though. Experimental data are also in good qualitative agreement with model predictions. The latter, nonetheless, seems to slightly underestimate the wave amplitude in the defocussing stage for collinear modulations.

For $k_0h < 1.36$, the modulation is suppressed for collinear perturbations and wave amplitude does not change significantly throughout the basin. This is predicted numerically and confirmed experimentally (see grey circles in Fig. 6). It is worth noting that the experimental set up assumes, *a priori*, an advanced stage of modulation as initial condition. Hence, during the first wavelengths of propagation, a defocussing takes place, reducing the extent of the modulation and wave amplitude. In the presence of oblique perturbations, on the other hand, wave packets remain unstable. Numerical simulations, in this respect, confirm that this instability still leads to the development of a robust wave amplification. Remarkably, this numerical result is qualitatively consistent with experimental observations (see black dashed line and squares in Fig. 6).

In conclusion, we have discussed a set of laboratory experiments in a large directional wave basin to investigate the instability of a sinusoidal (carrier) wave to oblique perturbations in finite water depth. Although modulational instability is suppressed for $k_0h < 1.36$ when propagation is restricted to one dimension, experiments show that perturbations propagating at an angle with the carrier waves can still trigger wave modulation, resulting in an amplitude growth (up to twice the amplitude of the carrier wave) also when $k_0h < 1.36$. Experimental evidence was supported and confirmed by direct numerical simulations of the Euler equations, which describes the evolution of the experimental wave packets under the effect of a four-wave interaction process only. The challenge now is to verify whether the instability to transverse perturbations can generate a notably large number of extreme waves also in more realistic random sea states.

This work has been supported by the European Community's Sixth Framework Programme through the grant to the budget of the Integrated Infrastructure Initiative HYDRALAB IV within the Transnational Access Activities, Contract No. 022441. F.W.O. Project G.0333.09 and E.U. Project EXTREME SEAS (Contract No. SCP8-GA-2009-234175) are also acknowledged. L.F. and J.M. acknowledge the Hercules Foundation and the Flemish Government department EWI for providing access to the Flemish Supercomputer Center. L.C. acknowledges the support of the MyWave EU funded FP7-SPACE-2011-1/CP-FP Project.

[1] A. Chabchoub, N. P. Hoffmann, and N. Akhmediev, "Rogue wave observation in a water wave tank," Phys. Rev. Lett. **106**(20), 204502 (2011).
[2] A. Chabchoub, N. Hoffmann, M. Onorato, and N. Akhmediev, "Super rogue waves: Observation of a higher-order breather in water waves," Phys. Rev. X **2**(1), 011015 (2012).
[3] M. Onorato, D. Proment, G. Clauss, and M. Klein, "Rogue waves: From nonlinear Schrödinger breather solutions to sea-keeping test," PLoS ONE **8**(2), e54629 (2013).
[4] D. Chalikov, "Freak waves: Their occurrence and probability," Phys. Fluids **21**, 076602 (2009).
[5] D. R. Solli, C. Ropers, P. Koonath, and B. Jalali, "Optical rogue waves," Nature (London) **450**, 1054–1057 (2007).
[6] B. Kibler, J. Fatome, C. Finot, G. Millot, F. Dias, G. Genty, N. Akhmediev, and J. M. Dudley, "The peregrine soliton in nonlinear fibre optics," Nat. Phys. **6**(10), 790–795 (2010).

[7] H. Bailung, S. K. Sharma, and Y. Nakamura, "Observation of peregrine solitons in a multicomponent plasma with negative ions," Phys. Rev. Lett. **107**, 255005 (2011).
[8] M. Onorato, S. Residori, U. Bortolozzo, A. Montina, and F. T. Arecchi, "Rogue waves and their generating mechanisms in different physical contexts," Phys. Rep. **528**(2), 47–89 (2013).
[9] P. A. E. M. Janssen, "Nonlinear four-wave interaction and freak waves," J. Phys. Oceanogr. **33**(4), 863–884 (2003).
[10] C. Kharif and E. Pelinovsky, "Physical mechanisms of the rogue wave phenomenon," Eur. J. Mech. B/Fluid **21**(5), 561–577 (2003).
[11] A. R. Osborne, *Nonlinear Ocean Waves and the Inverse Scattering Transform*, International Geophysics Series Volume 97 (Elsevier, San Diego, 2010).
[12] V. E. Zakharov and L. A. Ostrovsky, "Modulation instability: The beginning," Physica D **238**(5), 540–548 (2009).
[13] V. Zakharov, "Stability of period waves of finite amplitude on surface of a deep fluid," J. Appl. Mech. Tech. Phys. **9**, 190–194 (1968).
[14] A. R. Osborne, M. Onorato, and M. Serio, "The nonlinear dynamics of rogue waves and holes in deep-water gravity wave train," Phys. Lett. A **275**, 386–393 (2000).
[15] K. Dysthe, H. E. Krogstad, and P. Müller, "Oceanic rogue waves," Annu. Rev. Fluid Mech. **40**, 287–310 (2008).
[16] K. Trulsen, C. T. Stansberg, and M. G. Velarde, "Laboratory evidence of three-dimensional frequency downshift of waves in a long tank," Phys. Fluids **11**, 235 (1999).
[17] A. V. Babanin, T. Waseda, T. Kinoshita, and A. Toffoli, "Wave breaking in directional fields," J. Phys. Oceanogr. **41**(1), 145–156 (2011).
[18] K. Trulsen and K. B. Dysthe, "A modified nonlinear Schrödinger equation for broader bandwidth gravity waves on deep water," Wave Motion **24**, 281–289 (1996).
[19] K. Trulsen and K. B. Dysthe, "Frequency downshift in three-dimensional wave trains in a deep basin," J. Fluid Mech. **352**, 359–373 (1997).
[20] A. Slunyaev, C. Kharif, E. Pelinovsky, and T. Talipova, "Nonlinear wave focusing on water of finite depth," Physica D **173**(1–2), 77–96 (2002).
[21] F. R. S. Longuet-Higgins, "On the nonlinear transfer of energy in the peak of a gravity–wave spectrum: A simplified model," Proc. R. Soc. London, Ser. A **347**, 311–328 (1976).
[22] O. Gramstad and K. Trulsen, "Hamiltonian form of the modified nonlinear Schrödinger equation for gravity waves on arbitrary depth," J. Fluid Mech. **670**, 404–426 (2011).
[23] S. Haver and J. Andersen, "Freak waves: Rare realizations of a typical population or typical realizations of a rare population?" in *Proceedings of the 10th International Offshore and Polar Engineering (ISOPE) Conference*, Seattle, USA, May 2000.
[24] K. Trulsen, "Weakly nonlinear sea surface waves—Freak waves and deterministic forecasting," *Geometric Modelling, Numerical Simulation, and Optimization* (Springer, 2007), pp. 191–209.
[25] A. V. Babanin, T.-W. Hsu, A. Roland, S.-H. Ou, D.-J. Doong, and C. C. Kao, "Spectral wave modelling of typhoon krosa," Nat. Hazards Earth Syst. Sci. **11**(2), 501–511 (2011).
[26] H. Chien, C.-C. Kao, and L. Z. H. Chuang, "On the characteristics of observed coastal freak waves," Coast. Eng. Japan **44**(04), 301–319 (2002).
[27] T. B. Benjamin, "Instability of periodic wave trains in nonlinear dispersive systems," Proc. R. Soc. London **A299**, 59–75 (1967).
[28] D. J. Benney and G. J. Roskes, "Wave instabilities," Stud. Appl. Math. **48**(377), 377–385 (1969).
[29] G. B. Whitham, *Linear and Nonlinear Waves* (Wiley Interscience, New York, 1974).
[30] P. A. E. M. Janssen and M. Onorato, "The intermediate water depth limit of the Zakharov equation and consequences for wave prediction," J. Phys. Oceanogr. **37**, 2389–2400 (2007).
[31] Ø. Kristiansen, D. Fructus, D. Clamond, and J. Grue, "Simulations of crescent water wave patterns on finite depth," Phys. Fluids **17**, 064101 (2005).
[32] M. Francius and C. Kharif, "Three dimensional instabilities of periodic gravity waves in shallow water," J. Fluid Mech. **561**, 417–437 (2006).
[33] J. W. McLean, "Instabilities of finite-amplitude gravity waves on water of finite depth," J. Fluid Mech. **114**(1), 331–341 (1982).
[34] M. Onorato, L. Cavaleri, S. Fouques, O. Gramstad, P. A. E. M. Janssen, J. Monbaliu, A. R. Osborne, C. Pakozdi, M. Serio, C. T. Stansberg, A. Toffoli, and K. Trulsen, "Statistical properties of mechanically generated surface gravity waves: A laboratory experiment in a 3d wave basin," J. Fluid Mech. **627**, 235–257 (2009).
[35] B. J. West, K. A. Brueckner, R. S. Jand, D. M. Milder, and R. L. Milton, "A new method for surface hydrodynamics," J. Geophys. Res. **92**(C11), 11803–11824, doi:10.1029/JC092iC11p11803 (1987).
[36] A. Toffoli, M. Benoit, M. Onorato, and E. M. Bitner-Gregersen, "The effect of third-order nonlinearity on statistical properties of random directional waves in finite depth," Nonlinear Processes Geophys. **16**, 131–139 (2009).
[37] M. Tanaka, "Verification of Hasselmann's energy transfer among surface gravity waves by direct numerical simulations of primitive equations," J. Fluid Mech. **444**, 199–221 (2001).
[38] A. Toffoli, O. Gramstad, K. Trulsen, J. Monbaliu, E. M. Bitner-Gregersen, and M. Onorato, "Evolution of weakly nonlinear random directional waves: Laboratory experiments and numerical simulations," J. Fluid Mech. **664**, 313–336 (2010).
[39] E. Lo and C. C. Mei, "Numerical study of water-wave modulation based on a higher-order nonlinear Schrödinger equation," J. Fluid Mech. **150**(3), 395–416 (1985).
[40] M. P. Tulin and T. Waseda, "Laboratory observation of wave group evolution, including breaking effects," J. Fluid Mech. **378**, 197–232 (1999).